



HAL
open science

Motion-based ground reaction forces and moments prediction method for interaction with a moving and/or non-horizontal structure

Louise Demestre, Pauline Morin, François May, Nicolas Bideau, Guillaume Nicolas, Charles Pontonnier, Georges Dumont

► To cite this version:

Louise Demestre, Pauline Morin, François May, Nicolas Bideau, Guillaume Nicolas, et al.. Motion-based ground reaction forces and moments prediction method for interaction with a moving and/or non-horizontal structure. *Journal of Biomechanical Engineering*, 2022, pp.1-9. 10.1115/1.4054835 . hal-03691680

HAL Id: hal-03691680

<https://inria.hal.science/hal-03691680v1>

Submitted on 9 Jun 2022

HAL is a multi-disciplinary open access archive for the deposit and dissemination of scientific research documents, whether they are published or not. The documents may come from teaching and research institutions in France or abroad, or from public or private research centers.

L'archive ouverte pluridisciplinaire **HAL**, est destinée au dépôt et à la diffusion de documents scientifiques de niveau recherche, publiés ou non, émanant des établissements d'enseignement et de recherche français ou étrangers, des laboratoires publics ou privés.

Motion-based ground reaction forces and moments prediction method for interaction with a moving and/or non-horizontal structure

Louise Demestre *

IRISA - UMR 6074
Univ Rennes
35000 Rennes
France

Email: louise.demestre@ens-rennes.fr

Pauline Morin

IRISA - UMR 6074
Univ Rennes
35000 Rennes
France

Email: pauline.morin@ens-rennes.fr

François May

IRISA - UMR 6074
Univ Rennes
35000 Rennes
France

Email: francois.may@ens-rennes.fr

Nicolas Bideau

Inria, M2S
Univ Rennes
35000 Rennes
France

Email: nicolas.bideau@univ-rennes2.fr

Guillaume Nicolas

Inria, M2S
Univ Rennes
35000 Rennes
France

Email: guillaume.nicolas@univ-rennes2.fr

Charles Pontonnier

IRISA - UMR 6074
Univ Rennes
35000 Rennes
France

Email: charles.pontonnier@irisa.fr

Georges Dumont

IRISA - UMR 6074
Univ Rennes
35000 Rennes
France

Email: georges.dumont@irisa.fr

*Address all correspondence to this author.

Inverse dynamics methods are commonly used for the biomechanical analysis of human motion. External forces applied on the subject are required as an input data to solve the dynamic equilibrium of the subject. Force platforms measure ground reaction forces and moments (GRF&Ms) but they limit the ecological aspect of experimental conditions. Motion-based GRF&Ms prediction may circumvent this limitation. The current study aims at evaluating the accuracy of an optimization-based GRF&Ms prediction method modified to be applied to the interaction with a MNHS. The main improvement of the method deals with the contact detection in such a moving and/or non-horizontal frame. To evaluate the accuracy of the method, 20 subjects performed squats and steps on an instrumented moving structure, measuring both motion and GRF&Ms. The comparison of the root mean square error between the predicted and measured GRF&Ms divided by the subjects mass showed a similar order of magnitude than those from the method without the studied modification (0.14 N/kg for antero-posterior forces, 0.29 N/kg for medio lateral forces, 0.61 N/kg for longitudinal forces, 0.06 Nm/kg for frontal moments, 0.13 Nm/kg for sagittal moments, and 0.03 Nm/kg for transverse moments). The results showed the suitability of the method to study human motions for tasks performed on a MNHS.

1 Introduction

Inverse dynamics methods are widely used in motion analysis studies to calculate biomechanical variables from motion capture data [1]. The ground reaction forces and moments (GRF&Ms) are required to solve the dynamic equations from the subject's biomechanical model. The force platform is the gold standard for measuring GRF&Ms but it constrains the motion to a very limited capture area, reducing the ecological aspect of the experiment. Motion-based GRF&Ms prediction methods can be used to circumvent this limitation.

Inverse dynamics problems involving multiple contacts are underdetermined. Three motion-based approaches have been proposed in the literature to solve this problem: analytical, machine learning, and optimization approaches.

First, the analytical approach distributes global GRF&Ms among multiple contact points or predicts GRF&Ms at each contact point [2] using analytical relationships between external forces and kinematic variables. Global GRF&Ms are distributed between the two feet during double-stance phases based on the timing of the gait cycle [3, 4] or the position of the zero moment point [5]. This approach has only been applied to walking analysis.

Second, the machine learning approach uses statistical learning theory. Machine learning-based prediction methods often use neural networks (NNs). A NN is trained on motion capture and force sensor data to reproduce the relationship between kinematic parameters and GRF&Ms [6]. However, this approach requires a large amount of data [7] and each model is trained for a specific task. The average model determined is independent of individual specifics. In addition, the selection of input data depends on the study. For exam-

ple, a 2D study limited to the lower limbs requires a limited input [8].

Finally, the optimization approach distributes GRF&Ms by minimizing a cost function depending on the external forces, constrained by the dynamic equilibrium of the subject. Contact surfaces [9] or a set of discrete contact points [2, 10–14] are considered to simulate the contact. These methods have demonstrated their ability to predict external forces when studying various motions and subjects.

All of these methods assume that the ground is a static, horizontal surface. When a subject is interacting with a moving and/or non-horizontal structure (MNHS), measurement of external forces may be difficult or impossible. Many sports and work activities involve this type of interaction, such as working on a lifting platform, skateboarding, or skiing on a slope. Studies of human postural control also require the use of moving structures [15, 16]. Thus, a GRF&Ms prediction method adapted to tasks involving interaction between a human subject and a MNHS could further the biomechanical analysis of human motion for these applications. GRF&Ms prediction for such applications presents two challenges: accounting for the dynamics of the structure during the GRF&Ms prediction process [15, 16] and detecting contact between the structure and the subject's feet.

The purpose of this study is to evaluate the accuracy of an optimization-based GRF&Ms prediction method ([13], referred to as the "original method" hereafter) improved for application to interaction with a MNHS. The contact detection process of the original method was improved to account for contact with a MNHS. To evaluate the accuracy of the method, a moving structure equipped with force platforms, measuring GRFs&Ms applied to the subjects' feet, was used in synchronization with the motion capture. The measured GRF&Ms were compared with those predicted by the method proposed in this study. The experimental procedures, the GRF&Ms prediction method and the accuracy evaluation are presented. The results are then presented and discussed, with emphasis on the contact detection process under such ecological conditions.

2 Material and Methods

2.1 Experimental Procedures

Motion capture data were recorded using the optoelectronic system Qualisys (composed of 22 12 Mpixels OQUS 7+ cameras, 200 Hz). 6 female and 14 male subjects (age: 29 ± 9 years old, height: 180 ± 10 cm, mass: 70 ± 10 kg) participated in this study. This study was approved by the National INRIA Ethics Committee (Comité Opérationnel d'Évaluation des Risques Légaux et Éthiques, 2021-06, 02/22/2021), and all subjects signed an informed consent form.

During the experiment, the subjects performed different tasks while standing on two force platforms (one for each foot). These force platforms were composed of one lower steel plate (the same for both platforms), a 6-degrees-of-freedom strain-gauge force sensor (MCS10 5kN, 200 Hz, precision up to accuracy class 0.1, HBM, Germany) for each platform and an upper steel plate for each platform. The two

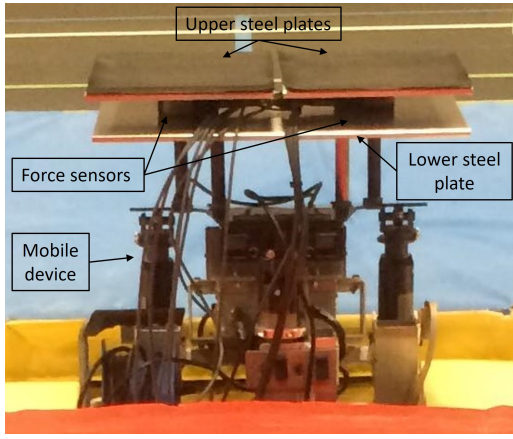


Fig. 1. Force platforms fixed on the mobile device

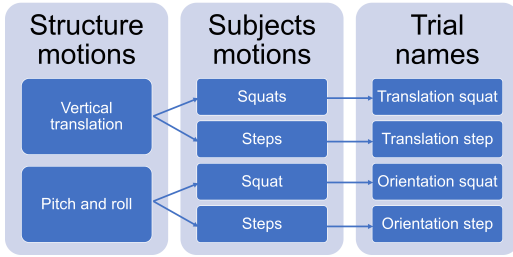


Fig. 2. Trials architecture

upper steel plates were covered with non-slip coating. The force platforms were fixed on a mobile device provided by CL Corporation (SASU, France) (Fig. 1).

A set of 45 reflective markers was placed on standardized anatomical landmarks as recommended by the International Society of Biomechanics [17, 18]. 3 additional markers were placed in corners of the lower steel plate of the force platforms.

A range of motion (sequential activation of each of the joints) was carried out. This trial was used to geometrically scale the model to the subject.

After a training phase to help the subjects feel comfortable on the mobile structure, the subjects performed 20 trials (5 repetitions of 4 motion combinations, Fig. 2).

The mobile structure was programmed to achieve different motions. Firstly, a motion (called Translation) was programmed: the mobile structure shifted up and then down with a maximal displacement of 0.032 m reached after 2.5 s. The motion of the mobile structure followed a trapezoidal velocity control law to reach a maximal velocity of 0.016 m.s⁻¹. Secondly, the mobile structure was programmed to perform a movement with combined pitch and roll components (called Orientation). The mobile structure repeated the same continuous back and forth 3D movement between an initial position and a final position, which lasted 7 s.

In combination with those programmed motions, the subject was asked to perform two types of tasks. The first, called Step, consisted of lifting up both feet successively twice during the mobile structure motion. The second, called Squat, consisted of performing two squats during the mobile



Fig. 3. PP defined on the biomechanical model. Issued from [13]

structure motion.

The combination of both subject and mobile structure motions resulted in 4 motion combinations: Translation Step, Translation Squat, Orientation Step and Orientation Squat. One video for each type of trial is available as supplementary material.

6 out of 400 trials were removed from this study due to forces sensors dysfunction or occlusion of the mobile structure markers.

2.2 GRF&Ms Prediction Method

The GRF&Ms were predicted using an improved version of the method presented by [13] for application to interaction with a MNHS. A biomechanical model with 18 segments, 18 joints and 44 degrees of freedom) was used. The subject-specific geometric calibration was realized with the method proposed in [19]. The inertial parameters of the body segments were computed from [20]. The inverse kinematics step to compute joint coordinates q consisted of an optimization approach based on Levenberg-Marquardt algorithm minimizing the least-squares distance between the experimental markers and those of the model [21]. The positions of the subject markers and mobile structure markers were filtered with 4th-order Butterworth low-pass filters with no phase shift and cutoff frequencies of 5 Hz and 4 Hz respectively. A cutoff frequency of 5 Hz was found to be suitable for non-rapid human motions [22] and a cutoff frequency of 4 Hz was used to study translation and rotation motions of a moving platform in [16]. The average reconstruction error was 1.42 ± 0.3 cm, taking into account the 394 trials.

Contact under the subject's feet was considered possible at a set of 28 (14 for each foot) discrete contact points on the biomechanical model, named prediction points (PP) (Fig. 3). The GRF&Ms prediction consisted of two steps at each frame: contact detection and forces distribution.

Firstly, a moving frame (O_m, X_m, Y_m, Z_m) linked to the mobile structure was created using the 3D displacements of the 3 markers placed on the lower steel plate of the force platforms, named $PL1$, $PL2$, and $PL3$ (Fig. 4). The marker $PL1$ was considered as the origin of the moving frame O_m . The X_m axis was defined by the normalized vector from $PL2$ to $PL1$. The vector from $PL3$ to the nearest mobile structure marker (here $PL2$) was used to define the plane of the mobile structure and its width W . Z_m was obtained from the cross product between the two previous vectors. Then, Z_m was normalized. Y_m was computed from the cross product between X_m and Z_m . The transformation matrix T from

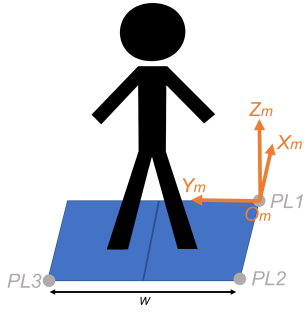


Fig. 4. Moving frame (O_m, X_m, Y_m, Z_m) linked to the moving structure

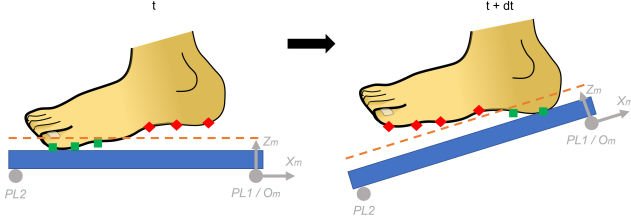


Fig. 5. Contact detection process in a moving frame (position threshold - dashed line, active contact points - square, inactive contact points in diamond, mobile structure markers in round)

the global frame to the moving frame was computed at each frame. The position of each PP was expressed in the moving frame using T . The relative velocity of each PP in the moving frame was defined as the difference between the absolute velocity of the PP and the absolute velocity of O_m , and was thus expressed in the global frame.

Contact was considered active when the corresponding PP respected all the following conditions (Fig. 5):

- a position according to Y_m between 0 m and W ,
- a position according to Z_m less than 0.02 m (to ensure that the PP was close enough to the ground),
- a relative velocity norm less than $0.8 \text{ m}\cdot\text{s}^{-1}$ (to ensure that the PP was almost without motion) [10].

On each active PP a 3-component force was considered. This force was limited to 0.4 Body Weight [10] and had to respect the Coulomb's friction law (friction coefficient of 0.5) [11]. Secondly, the quadratic sum of the external forces applied to each active PP was minimized with respect to the dynamic equilibrium of the subject. At each frame, the optimization problem presented in Eqn. (1) was solved using a Sequential Quadratic Programming method [13].

$$\begin{aligned} \min_F \quad & \sum_{i=1}^{i=28} \|F_i\|^2 \\ \text{s. t.} \quad & \begin{cases} M(q)\ddot{q} + C(q, \dot{q}) + G(q) + \lambda + E = 0 \\ \forall i \in \llbracket 1, 28 \rrbracket, F_i \leq F_i^{\max} \end{cases} \end{aligned} \quad (1)$$

Where, isolating the biomechanical model, $M(q)$ is the

inertia matrix, $C(q, \dot{q})$ is the centrifugal and Coriolis force vector, $G(q)$ is the gravity force vector, λ is the generalized internal force vector, E is the generalized external force vector, and F_i^{\max} is the vector containing the maximal forces available for the PP i . The external force vector E contains the external efforts F_i applied on the PP i .

The prediction method in a moving frame was implemented in the CusToM Matlab toolbox [23] and all the computations were performed using this toolbox.

Each upper steel plate of the mobile platform had a weight $m = 2.6 \text{ kg}$. For Translation trials, the vertical velocity profile was considered to be a perfect trapeze. The vertical acceleration obtained was $\gamma = 0.032 \text{ m}\cdot\text{s}^{-2}$. An estimation of the angular acceleration according to X_m during the Orientation trials was made. The other angular accelerations were considered to be of the same order of magnitude. Each upper steel plate of the mobile platform had a moment of inertia $I = 0.013 \text{ kg}\cdot\text{m}^2$. The motion of the mobile device came from 3 translational actuators. The 2 actuators in the plan (O_m, Y_m, Z_m) were considered to be moving in the opposite direction with a vertical acceleration γ . The angular acceleration obtained from these assumptions was $\omega = 0.18 \text{ rad}\cdot\text{s}^{-2}$. From all these quantities, the following results were calculated:

- $m\gamma = 0.08 \text{ N}$,
- $I\omega = 0.002 \text{ Nm}$.

So, the inertial components of the moving structure were considered as negligible with respect to the subject's weight.

2.3 Data Analysis

Predicted and measured GRF&Ms were compared using root mean square error divided by subject's mass (RMSE/m) and relative RMSE (rRMSE) [24]. The RMSE between the predicted and measured CoP positions (RMSE CoP) were also computed. To compute the CoP positions, the predicted and measured GRF&Ms were expressed in the moving frame linked to the mobile structure. In this frame, the CoP was regarded as the point at zero altitude where the F and S moments were zero. The CoP positions were computed only when the norm of the GRF were over 10 % of the BW to avoid unusable results when the contact between the foot and ground was lost. All the metrics were computed for each subject, each trial, each GRF&M component, and each foot. The RMSE and rRMSE were defined as in Eqn. (2) and Eqn. (3) respectively:

$$\text{RMSE} = \sqrt{\frac{1}{D} \sum_{t=0}^{t=T} (u_1(t) - u_2(t))^2} \quad (2)$$

$$\text{rRMSE} = \frac{\text{RMSE}}{\frac{1}{2} \sum_{i=1}^{i=2} \left(\max_{t \in [0, T]} u_i(t) - \min_{t \in [0, T]} u_i(t) \right)} \quad (3)$$

where D is the duration of the trial, $u_1(t)$ and $u_2(t)$ are the predicted force or moment and the measured one respectively. RMSE/mass, rRMSE and RMSE CoP were averaged across all subjects, all trials and both feet to provide an overview of the accuracy. The mean and standard deviation values of RMSE/mass, rRMSE were also calculated for each type of trial separately.

To validate the presented method accuracy, comparisons with similar results from literature were carried out. Some tasks studied in the literature were not taken into account because the motions were considered to be too different from those studied in the present article. Reference [13] studied asymmetric handling tasks with different loads. Only the case without any load was considered. Reference [10] studied walking at different speeds, walking over different obstacles, gait initiation, gait termination, deep squatting, and stair ascent and descent. Only walking at different speeds, deep squatting, and stair ascent and descent were taken into account. Reference [2] studied human walking at different speed and running. Only the results for walking at different speeds were taken into account.

The different components of forces and moments were named as follows:

- AP for antero-posterior forces,
- ML for medio-lateral forces,
- L for longitudinal forces,
- F for frontal moments,
- S for sagittal moments,
- T for transverse moments.

3 Results

The averaged RMSE/m and rRMSE for the presented method are presented in Tab. 1 for forces and Tab. 2 for moments. The RMSE CoP are presented in Tab. 2.

The RMSE/m obtained from the presented method were of the same order of magnitude as those from [13] and [10] for all the force components except for L (0.61 for the presented method and 0.25 for [13]). There were lower than those from [2]. The rRMSE obtained from the presented method were of the same order of magnitude as those obtained from [13] for all force components.

The RMSE/m and rRMSE obtained from the presented method were lower or of the same order of magnitude as [13] and [10] for all moment components. The RMSE CoP obtained from the presented method were higher than those obtained from [2].

Figures 6 to 9 present examples of the predicted and measured GRF&Ms divided by the subject's mass for the left

foot for each type of trial. For the medio-lateral forces, there was an offset between the predicted and measured curves during the static phases (colored shapes). The predicted efforts were close to zero, which was not the case for the measured ones. This type of offset was not visible during the Translation Step trial (static phase was between 2 s and 5 s).

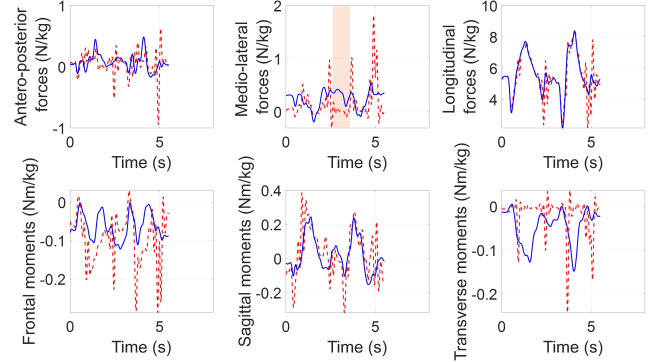


Fig. 6. Example of the predicted (dashed line) and measured (solid line) GRF&Ms divided by the subject's mass for a Translation Squat trial (left foot). Scales of the ordinate-axis are different between the 6 graphs. The offsets due to a static phase are visible in the colored shapes

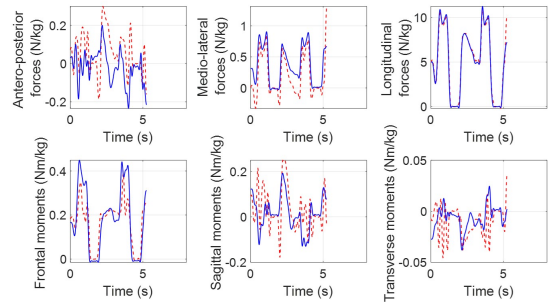


Fig. 7. Example of the predicted (dashed line) and measured (solid line) GRF&Ms divided by the subject's mass for a Translation Step trial (left foot). Scales of the ordinate-axis are different between the 6 graphs

The RMSE/m and the rRMSE are for each type of trials are presented in Tab. 3. For a given force component and subject's movement, the different results are similar. So, it seemed that results were unrelated to the mobile structure motion. The type of subject's motion seemed to have an impact on the results. The AP and ML forces, and S moments presented higher RMSE/m for trials involving squats than for trials involving steps. The ML and L forces, and F and T moments presented higher rRMSE for trials involving squats than for trials involving steps.

Table 1. Averaged RMSE/m and rRMSE, and associated standard deviation in parentheses for forces

Components	AP		ML		L	
	RMSE/m (N/kg)	rRMSE	RMSE/m (N/kg)	rRMSE	RMSE/m (N/kg)	rRMSE
Presented method	0.14 (0.07)	0.20 (0.07)	0.29 (0.09)	0.25 (0.12)	0.61 (0.25)	0.09 (0.06)
[13]	0.09 (0.07)	0.17 (0.14)	0.40 (0.32)	0.38 (0.29)	0.25 (0.23)	0.03 (0.03)
[2]	1.21 (0.18)	-	0.57 (0.11)	-	2.58 (0.43)	-
[10]	0.31 (0.09)	-	0.23 (0.09)	-	0.72 (0.20)	-

Table 2. Averaged RMSE/m, rRMSE and RMSE CoP, and associated standard deviation in parentheses for moments

Components	F			S			T	
	RMSE/m (Nm/kg)	rRMSE	RMSE CoP (mm)	RMSE/m (Nm/kg)	rRMSE	RMSE CoP (mm)	RMSE/m (Nm/kg)	rRMSE
Presented method	0.06 (0.02)	0.22 (0.09)	47.6 (108)	0.13 (0.03)	0.20 (0.07)	17.0 (48)	0.03 (0.02)	0.32 (0.13)
[13]	0.09 (0.08)	0.17 (0.15)	-	0.14 (0.11)	0.13 (0.10)	-	0.10 (0.07)	0.57 (0.41)
[2]	-	-	24.6 (5.0)	-	-	9.2 (4.0)	-	-
[10]	0.12 (0.04)	-	-	0.18 (0.05)	-	-	0.18 (0.06)	-

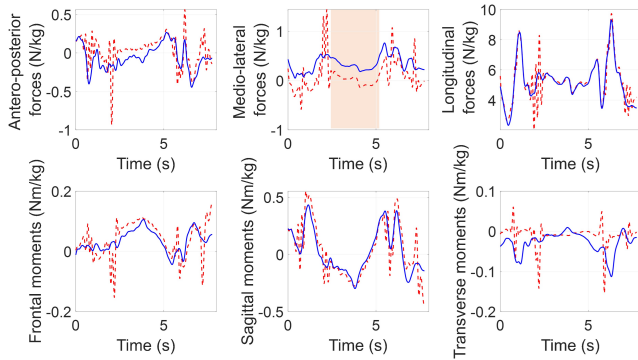


Fig. 8. Example of the predicted (dashed line) and measured (solid line) GRF&Ms divided by the subject's mass for an Orientation Squat trial (left foot). Scales of the ordinate-axis are different between the 6 graphs. The offsets due to a static phase are visible in the colored shapes

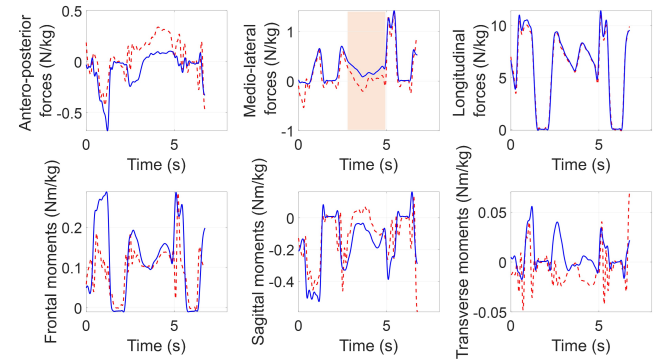


Fig. 9. Example of the predicted (dashed line) and measured (solid line) GRF&Ms divided by the subject's mass for an Orientation Step trial (left foot). Scales of the ordinate-axis are different between the 6 graphs. The offsets due to a static phase are visible in the colored shapes

4 Discussion

4.1 Method Accuracy

The presented method seemed to provide similar results to those from [13]. The difference between the presented method and the original method [13] was the contact detection step. So, it seemed that this modification did not have an impact on the accuracy of the overall method. The discrepancy observed for the RMSE/m for L was not significant due to the high magnitude of this component. As shown in Figures 6 to 9, L reached up to 11 N/kg. A RMSE/m of 0.61 N/kg can thus be considered negligible. This observation is confirmed by the rRMSE, which takes into account the maximum magnitude, and which was very low and similar to those from [13]. Moreover, all the metrics except those

based on the CoP positions were lower or in the same order of magnitude as those from [2, 10]. The RMSE CoP were approximately twice higher than those from [2]. This observation may come from the moving frame consideration, the computation of the predicted moments far from the contact point in our study, the used threshold of 10 % of BW in our study, and the CoP positions which were approximated to the moment divided by the vertical force in [2].

The observation of an offset between the predicted and measured GRF&Ms was also made in the study presenting the original method [13]. It is probably due to efforts generated by the subject to improve his stability but without influence on the subject's motion. For example, a similar offset was visible for the medio-lateral forces of the right

Table 3. Mean RMSE, RMSE/mass, rRMSE, and ρ and associated standard deviation in parentheses for each type of trials

GRF&M components	Type of trials	Left foot		Right foot	
		RMSE/mass N/kg or Nm/kg	rRMSE	RMSE/mass N/kg or Nm/kg	rRMSE
Antero-posterior forces	Translation Squat	0.19 (0.09)	0.21 (0.05)	0.18 (0.07)	0.23 (0.06)
	Translation Step	0.11 (0.03)	0.22 (0.06)	0.10 (0.03)	0.24 (0.08)
	Orientation Squat	0.16 (0.05)	0.16 (0.03)	0.14 (0.05)	0.17 (0.04)
	Orientation Step	0.10 (0.06)	0.15 (0.05)	0.10 (0.06)	0.15 (0.05)
Medio-lateral forces	Translation Squat	0.30 (0.08)	0.34 (0.10)	0.33 (0.09)	0.42 (0.17)
	Translation Step	0.22 (0.04)	0.18 (0.03)	0.24 (0.05)	0.24 (0.07)
	Orientation Squat	0.31 (0.07)	0.23 (0.05)	0.35 (0.09)	0.27 (0.08)
	Orientation Step	0.24 (0.09)	0.15 (0.03)	0.27 (0.10)	0.18 (0.04)
Longitudinal forces	Translation Squat	0.60 (0.30)	0.11 (0.07)	0.69 (0.28)	0.13 (0.06)
	Translation Step	0.62 (0.24)	0.06 (0.02)	0.65 (0.18)	0.06 (0.02)
	Orientation Squat	0.57 (0.24)	0.10 (0.05)	0.69 (0.25)	0.12 (0.06)
	Orientation Step	0.50 (0.25)	0.05 (0.02)	0.57 (0.24)	0.05 (0.02)
Frontal moments	Translation Squat	0.06 (0.02)	0.27 (0.10)	0.06 (0.03)	0.26 (0.10)
	Translation Step	0.07 (0.02)	0.23 (0.07)	0.06 (0.02)	0.19 (0.07)
	Orientation Squat	0.05 (0.01)	0.23 (0.07)	0.05 (0.02)	0.20 (0.07)
	Orientation Step	0.06 (0.02)	0.20 (0.07)	0.05 (0.01)	0.17 (0.06)
Sagittal moments	Translation Squat	0.15 (0.03)	0.23 (0.07)	0.14 (0.04)	0.23 (0.07)
	Translation Step	0.11 (0.02)	0.22 (0.06)	0.11 (0.02)	0.21 (0.06)
	Orientation Squat	0.13 (0.03)	0.18 (0.06)	0.13 (0.03)	0.18 (0.06)
	Orientation Step	0.11 (0.03)	0.19 (0.06)	0.10 (0.03)	0.17 (0.05)
Transverse moments	Translation Squat	0.05 (0.02)	0.39 (0.15)	0.05 (0.02)	0.45 (0.18)
	Translation Step	0.02 (0.00)	0.27 (0.07)	0.02 (0.01)	0.34 (0.09)
	Orientation Squat	0.04 (0.01)	0.28 (0.11)	0.04 (0.01)	0.33 (0.13)
	Orientation Step	0.02 (0.02)	0.24 (0.07)	0.02 (0.02)	0.26 (0.08)

foot but with an opposite value. So, both feet were pushing side-wards during standing, which was canceled out when summing the contributions from both feet. The optimization method would predict zero medio-lateral force, in this case, on both feet. Moreover, during the static phase of the trials involving steps, the subjects were standing on their two feet, which leads to an underdetermined problem. During the beginning and the end of the trials, the subjects were waiting for investigator's instructions while staying static. So these parts of the trials were removed to reduce the impact of this phenomenon on the results.

Comparing the RMSE/m and the rRMSE for each type of trial, it was found that the results were unrelated to the

mobile structure motion. A study with more challenging structure motions could be interesting to confirm this observation. It was also found that the trials involving squats led to higher errors than those involving steps. The distribution of the GRF&M on the two feet during the complete movement could be a source of errors. These considerations should be taken into account for other tasks involving GRF&M with double-contact phases.

In conclusion, the contact detection process for MNHS seemed to maintain the accuracy of the overall GRF&Ms prediction method.

4.2 Limits and Perspectives

The method presented in this study is based on several parameters such as the number of contact points, the position and velocity thresholds, the maximum force available at each point, the friction coefficient between the feet and the ground. These parameters were set using previous studies from the literature or empirical approaches [10,11,13]. It may be interesting to study the impact of these parameters on the method and to find the optimal setting that may depend on the subject and the task to be studied.

The proposed method is based on the minimization of external forces. The minima found with this method may generate very high internal forces. It could be interesting to use an objective function taking into account internal forces, or joint reaction forces or muscle forces to avoid unrealistic solutions. This could also compensate for the offset observed during static phases [11,25].

[2, 10, 13] and the presented methods all use the same concept of inverse dynamics-based optimization. [10] uses also a force shaping method to avoid discontinuities between single stance and double stance periods. This force shaping method may improve the presented method accuracy. A maximal force available at each contact point depending on their displacements and velocities [2] may also improve the presented method accuracy.

In this study, the foot was modelled as a single rigid body. The contact detection step was based on the foot model and not on the experimental markers. The reconstructed orientation of the foot model may be different from that of the real foot, especially due to the joint between the toes and the rest of the foot. So, some PP may have been considered inactive in the model but corresponded to a point which was in contact with the ground in reality. A more realistic foot model with 2 articulated segments (the toes and the rest of the foot) [9] could improve the contact detection step and avoid missing some active PP.

The method presented in this article aims at extending GRF&Ms prediction methods application scope to studies involving an interaction between the subject and a MNHS. The accelerations experienced by the mobile structure and the subjects during this experiment were lower than those involved in the targeted applications. This choice was made to ensure the safety of the subjects. So a new experimental set-up should be used to validate the accuracy of the presented method during tasks involving similar accelerations to those as in the targeted applications. Moreover, the higher accelerations of the moving structure will require the computation or compensation of inertial components of the mobile structure to get force platform data for validation of the methods for the targeted applications [15, 16, 26].

The application scope of this method could be extended to interaction with deformable structures such as springboards, uneven floors and ramps such as those used for sliding sports, and stairs. These floors and structures can be considered as a succession of rigid surfaces with different orientations. The method proposed in this study could be improved with a location of the contact surface among the whole floor or structure. The GRF&Ms prediction method

presented in this article could then be applied to studies involving interaction with the above mentioned structures. The high accelerations of a springboard will also require consideration of its inertial components for validation of the methods for this application.

The technology used to collect motion capture data is a limiting factor for the application scope. The capture volume is limited and constrains the area where the motion is tracked. It may be restricting for large displacement motions, which is the case for the study of skiing for example. Moreover, some of the targeted applications are performed outdoors. This is another difficulty for motion capture technology which is sensitive to light reflections. Some of the targeted applications involve small motions with high acceleration (skateboarding for example). For these tasks, the sampling frequency of the optoelectronic system used to collect motion capture data may be limiting (maximum 300 Hz with 12 Mpixels resolution and 1100 Hz with 3 Mpixels resolution for Qualisys) as well as its tracking accuracy (about 1 mm). It could be interesting to modify the method to adapt it to other types of input data (markerless technology, ...), keeping in mind that the motion of the MNHS interacting with the subject must be known.

5 Conclusions

This study showed that the accuracy of the GFR&M prediction method improved with a contact detection process adapted to MNHS was similar to that of the original method. This new method is based on motion capture data and only requires the use of additional markers to track motion of the MNHS.

It opens the application scope of biomechanical analysis based on inverse dynamics methods to sport activities such as skateboarding and working activities such as those performed on an elevating platform. A few improvements of the presented method could even extend the application scope to activities of daily living such as stair climbing or other sport activities such as sports involving a springboard (diving, athletics, gymnastics). A study on the inertial components of the mobile structure should be carried out to evaluate the accuracy of the presented method for the targeted applications.

6 Acknowledgements

The authors would like to thank Antoine Muller for his help in analysing the results and comparing them with the literature, and Claire Livet for her help for computing the different results.

References

- [1] Erdemir, A., McLean, S., Herzog, W., and van den Bogert, A. J., 2007. "Model-based estimation of muscle forces exerted during movements". *Clinical Biomechanics*, **22**(2), feb, pp. 131–154.
- [2] Jung, Y., Jung, M., Ryu, J., Yoon, S., Park, S.-K., and Koo, S., 2016. "Dynamically adjustable foot-ground

- contact model to estimate ground reaction force during walking and running”. *Gait and Posture*, **45**, pp. 62–68.
- [3] Koopman, B., Grootenboer, H. J., and de Jongh, H. J., 1995. “An inverse dynamics model for the analysis, reconstruction and prediction of bipedal walking”. *Journal of Biomechanics*, **28**(11), nov, pp. 1369–1376.
- [4] Karatsidis, A., Bellusci, G., Schepers, H. M., de Zee, M., Andersen, M. S., and Veltink, P. H., 2017. “Estimation of ground reaction forces and moments during gait using only inertial motion capture”. *Sensors (Switzerland)*, **17**(1), jan, p. 75.
- [5] Dijkstra, E. J., and Gutierrez-Farewik, E. M., 2015. “Computation of ground reaction force using Zero Moment Point”. *Journal of Biomechanics*, **48**(14), pp. 3776–3781.
- [6] Oh, S. E., Choi, A., and Hwan Mun, J., 2013. “Prediction of ground reaction forces during gait based on kinematics and a neural network model”. *Journal of Biomechanics*, **46**, pp. 2372–2380.
- [7] Johnson, W. R., Alderson, J., Lloyd, D., and Mian, A., 2019. “Predicting athlete ground reaction forces and moments from spatio-temporal driven CNN models”. *IEEE Transactions on Biomedical Engineering*, **66**(3), pp. 689–694.
- [8] Lim, H., Kim, B., and Park, S., 2020. “Prediction of lower limb kinetics and kinematics during walking by a single IMU on the lower back using machine learning”. *Sensors (Switzerland)*, **20**(1), jan, p. 130.
- [9] Van Hulle, R., Schwartz, C., Denoël, V., Croisier, J. L., Forthomme, B., and Brüls, O., 2020. “A foot/ground contact model for biomechanical inverse dynamics analysis”. *Journal of Biomechanics*, **100**, p. 109412.
- [10] Fluit, R., Andersen, M. S., Kolk, S., Verdonshot, N., and Koopman, H. F., 2014. “Prediction of ground reaction forces and moments during various activities of daily living”. *Journal of Biomechanics*, **47**(10), pp. 2321–2329.
- [11] Skals, S., Jung, M. K., Damsgaard, M., and Andersen, M. S., 2017. “Prediction of ground reaction forces and moments during sports-related movements”. *Multibody System Dynamics*, **39**(3), pp. 175–195.
- [12] Muller, A., Pontonnier, C., Robert-Lachaine, X., Dumont, G., and Plamondon, A., 2020. “Motion-based prediction of external forces and moments and back loading during manual material handling tasks”. *Applied Ergonomics*, **82**, jan, p. 102935.
- [13] Muller, A., Pontonnier, C., and Dumont, G., 2020. “Motion-based prediction of hands and feet contact efforts during asymmetric handling tasks”. *IEEE Transactions on Biomedical Engineering*, **67**(2), pp. 344–352.
- [14] Jung, Y., Jung, M., Lee, K., and Koo, S., 2014. “Ground reaction force estimation using an insole-type pressure mat and joint kinematics during walking”. *Journal of Biomechanics*, pp. 2693–2699.
- [15] Preuss, R., and Fung, J., 2004. “A simple method to estimate force plate inertial components in a moving surface”. *Journal of Biomechanics*, **37**(8), pp. 1177–1180.
- [16] Roberts, B. W., Hall, J. C., Williams, A. D., Rouhani, H., and Vette, A. H., 2019. “A method to estimate inertial properties and force plate inertial components for instrumented platforms”. *Medical Engineering and Physics*, **66**, pp. 96–101.
- [17] Wu, G., Siegler, S., Allard, P., Kirtley, C., Leardini, A., Rosenbaum, D., Whittle, M., D D’Lima, D., Cristofolini, L., Witte, H., Schmid, O., and Stokes, I., 2002. “ISB recommendation on definitions of joint coordinate system of various joints for the reporting of human joint motion—part I: ankle, hip, and spine”. *Journal of Biomechanics*, **35**(4), pp. 543–548.
- [18] Wu, G., Van Der Helm, F. C., Veeger, H. E., Makhsous, M., Van Roy, P., Anglin, C., Nagels, J., Karduna, A. R., McQuade, K., Wang, X., Werner, F. W., and Buchholz, B., 2005. “ISB recommendation on definitions of joint coordinate systems of various joints for the reporting of human joint motion - Part II: Shoulder, elbow, wrist and hand”. *Journal of Biomechanics*, **38**(5), pp. 981–992.
- [19] Muller, A., Germain, C., Pontonnier, C., and Dumont, G., 2015. “A simple method to calibrate kinematical invariants: application to overhead throwing”. In Proc. 33rd International Conference of International Society of Biomechanics in Sports (ISBS), pp. 2–5.
- [20] Dumas, R., Chèze, L., and Verriest, J.-P., 2007. “Adjustments to McConville et al. and Young et al. body segment inertial parameters”. *Journal of Biomechanics*, **40**, pp. 543–553.
- [21] Lu, T. W., and O’Connor, J. J., 1999. “Bone position estimation from skin marker co-ordinates using global optimisation with joint constraints”. *Journal of Biomechanics*, **32**(2), feb, pp. 129–134.
- [22] Skogstad, S. A., Høvin, M., Holm, S., Jensenius, A. R., and Nymo, K., 2013. “Filtering Motion Capture Data for Real-Time Applications”.
- [23] Muller, A., Pontonnier, C., Puchaud, P., and Dumont, G., 2019. “CusToM: a Matlab toolbox for musculoskeletal simulation”. *Journal of Open Source Software, Open Journals*, **4**(33), pp. 1–3.
- [24] Ren, L., Jones, R. K., and Howard, D., 2008. “Whole body inverse dynamics over a complete gait cycle based only on measured kinematics”. *Journal of Biomechanics*, **41**(12), pp. 2750–2759.
- [25] Morin, P., Muller, A., Pontonnier, C., and Dumont, G., 2021. “Studying the impact of internal and external forces minimization in a motion-based external forces and moments prediction method: application to fencing lunges”. In ISB 2021-XXVIII Congress of the International Society of Biomechanics, p. 1.
- [26] Hnat, S. K., van Basten, B. J., and van den Bogert, A. J., 2018. “Compensation for inertial and gravity effects in a moving force platform”. *Journal of Biomechanics*, **75**, jun, pp. 96–101.